Morphological and transcriptomic evidence for ammonium induction of sexual reproduction in *Thalassiosira pseudonana* and other centric diatoms

Eric R. Moore[1], Briana S. Bullington[1], Alexandra J. Weisberg[2], Yuan Jiang[3], Jeff Chang[2], Kimberly H. Halsey[1]*

[1]Department of Microbiology, Oregon State University, Corvallis, Oregon 97331, USA

[2]Department of Botany and Plant Pathology, Oregon State University, Corvallis, Oregon 97331, USA

[3]Department of Statistics, Oregon State University, Corvallis, Oregon 97331, USA

* Corresponding Author

E-mail: halseyk@science.oregonstate.edu (KHH)

Abstract

The reproductive strategy of diatoms includes asexual and sexual phases, but in many species, including the model centric diatom *Thalassiosira pseudonana*, sexual reproduction has never been observed. Furthermore, the environmental factors that trigger sexual reproduction in diatoms are not understood. Although genome sequences of a few diatoms are available, little is known about the molecular basis for sexual reproduction. Here we show that ammonium reliably induces the key sexual morphologies, including oogonia, auxospores, and spermatogonia, in two strains of *T. pseudonana*, *T. weissflogii*, and *Cyclotella cryptica*. RNA sequencing revealed 1,274 genes whose expression patterns changed when *T. pseudonana* was induced into sexual reproduction by ammonium. Some of the induced genes are linked to meiosis or encode flagellar structures of heterokont and cryptophyte algae. The identification of ammonium as an environmental trigger suggests an unexpected link between diatom bloom dynamics and strategies for enhancing population genetic diversity.

Introduction

Diatoms are protists that form massive annual spring and fall blooms in aquatic environments and are estimated to be responsible for about half of photosynthesis in the global oceans [1]. This predictable annual bloom dynamic fuels higher trophic levels and initiates delivery of carbon into the deep ocean biome. Diatoms have complex life history strategies that are presumed to have contributed to their rapid genetic diversification into ~200,000 species [2] that are distributed between the two major diatom groups: centrics and pennates [3]. A defining characteristic of all diatoms is their restrictive and bipartite silica cell wall that causes them to progressively shrink during asexual cell division. At a critically small cell size and under certain conditions, auxosporulation restitutes cell size and prevents clonal death [4-6]. The entire lifecycles of only a few diatoms have been described and rarely have sexual events been captured in the environment [7-9].

So far, all centric diatoms appear to share the process of oogamous sexual reproduction (Fig 1). The average cell size of a population of asexually dividing diatoms decreases as a result of differential thecae inheritance. At a critically small size, cells become eligible to differentiate into male and female cells. Meiosis in the male spermatogonangium produces multinucleate spermatogonia that divide into individual haploid spermatocytes. Meiosis in the female oogonia produces a single functional haploid nucleus that is fertilized by a flagellated spermatocyte through an opening in the oogonia thecae. Fertilized oogonia expand into a large auxospore where new, large thecae are formed for the new, enlarged initial cell. Auxosporulation can also occur asexually, but it is considered an ancillary pathway for cell size restitution in diatom species that have a sexual path for reproduction [5].

Fig 1. The life cycle of a centric diatom. The average cell size of a population of asexually dividing diatoms decreases as a result of differential thecae inheritance. At a critically small size, cells can initiate sexual reproduction and differentiate into male and female cells. Meiosis in the male spermatogonangium produces multinucleate spermatogonia that divide into individual haploid spermatocytes. Meiosis in the female oogonia produces a single functional haploid nucleus that is fertilized by a flagellated spermatocyte through an opening in the oogonia thecae. Fertilized oogonia expand into a large auxospore where new, large thecae are formed for the new initial cell.

The environmental factors that trigger formation of sexual cells and sexual reproduction in centric diatoms are not well understood [10, 11], but sexualization appears to be strongly associated with conditions causing synchronous sexuality in cells experiencing growth stress [12]. Besides the size threshold requirement, previous observations indicate that sexualization is possible when active growth has ceased, causing cell cycle arrest [13, 14] and cell densities are sufficient to permit successful fertilization of the oogonia by the spermatocyte [15]. Light interruption with an extended dark period [13], changing salinities, and nutrient shifts [16], have sometimes been successful in inducing sexual reproduction, probably by causing cell cycle arrest. Recently, pheromones produced by the pennate diatom, *Seminavis robusta,* have been identified that cause cell cycle arrest and induce the sexual pathway [17]. However, we are aware of no method that reliably causes induction of all of the sexual stages of centric diatoms shown in figure 1.

The ecological importance of diatoms, combined with their potential uses in materials chemistry, drug delivery, biosensing [18, 19], and bioenergy [20, 21], prompted genome sequencing of *T. pseudonana* CCMP1335 (a 'centric' diatom collected from the North Atlantic Ocean) and *Phaeodactulum tricornutum* (a 'pennate' diatom), which have become model organisms for experimental studies [22, 23]. However, sexual morphologies have never been observed in either of these species or in the vast majority of diatoms [10]. The inability to reliably control the sexual cycle in centric diatoms has severely hindered studies to understand the silica deposition process, as well as the genetic regulation, ecology, and evolution of sex [10, 24, 25]. Both of the model diatoms were thought to have repurposed their extant genetic toolkits and lost the need and ability for a sexual lifestyle [10, 11, 26].

Here we show that two strains of *T. pseudonana* and two other centric species, *T. weisflogii* and *Cyclotella cryptica,* can be reliably induced into the sexual reproductive pathway when cells are below the critical size threshold and exposed to ammonium during the stationary phase of growth. Ammonium induced oogonia, auxospore, and spermatocyte formation in each of these species. Induction of sexuality was further supported by RNA sequencing (RNAseq) which revealed 1,274 genes whose expression patterns changed when *T. pseudonana* became sexualized by ammonium. Meiosis genes and genes associated with flagellar structures of heterokont and cryptophyte algae were differentially expressed in ammonium-induced cells compared to nitrate grown cells. We anticipate that this discovery will open opportunities to study the evolution of diatom lifecycles and facilitate expansion of diatom breeding to explore functional genetics for molecular ecology, nanotechnology and biofuels applications.

Results and discussion

Ammonium triggers sexual morphologies

We observed *T. pseudonana* CCMP1335 cell morphologies consistent with sexual reproduction when cells were propagated in artificial seawater medium supplemented with ammonium. The proportion of cells that differentiated into sexual cell types was dependent on ammonium concentration, with up to 39% of the population identified as oogonia or auxospores in cultures supplemented with 800 μM NH_4Cl (Fig 2A). Oogonia and auxospores were first observed at the onset of stationary phase and reached maximum population proportions in late stationary phase (Fig 2A). Ammonium also induced oogonia and auxospore production in *T. pseudonana* CCMP1015 (collected from the North Pacific Ocean), *T. weissflogii*, and *Cyclotella cryptica* (S1 Fig). A few oogonia and auxospores were observed in nitrate grown cultures with no added ammonium (Fig 2A and S1). However, with the exception of nitrate grown *C. cryptica* cultures, which generated oogonia and auxospores constituting 11% of the total population, oogonia and auxospores were only a small percentage of the total population in nitrate-grown *T. pseudonana* and *T. weissflogii.* Even though auxospores can have diameters 3-4 times that of asexual cells, such small population proportions do not lead to discernable shifts in cell size distributions obtained by particle size analysis (e.g., Coulter counter, a commonly used method to assess population size). We initially observed auxospores when performing visual inspections using a light microscope of our cultures that were growing in ammonium. For the data reported here, oogonia and auxospores were quantified by manually counting the cell types using a hemocytometer. We suspect that reliance on laboratory instruments such as particle counters and flow cytometers in place of microscopic analysis is one reason that sexual morphologies in these well-studied diatom species have gone undetected until now. Laboratory stock cultures are

typically maintained in media with low concentrations of nitrogen, especially when ammonium is supplied as the nitrogen source because it has been considered to be toxic to diatoms in high concentrations [27]. Therefore, it may not be surprising that sexual cells have gone un-noticed due to the low rates of sexual induction in the presence of low ammonium concentrations (Fig. 2A).

Fig 2. Ammonium induces sexual morphologies in *T. pseudonana* CCMP1335. (**A)** Proportion of sexual cells (oogonia and auxospores) relative to the total population in cultures of *T. pseudonana* grown in the presence of NH_4Cl or $NaNO_3$; n=3 independent cultures, average of 300 cells counted per replicate. Oogonia and auxospores were only observed beginning in stationary phase, data are mean values, error bars are s.d.. Inset: corresponding growth curve linking the onset of stationary phase with first appearance of sexual cells on day six. (**B)** Sexual cells were observed in cultures with NH_4Cl present at inoculation (blue hatched and solid blue bars) or following NH_4Cl addition at the onset of stationary phase (yellow bars). Legend shows concentration of nitrogen source provided at inoculation and concentration of nitrogen source added at the time of the second dosing. Two control treatments were supplied 200 μM nitrogen source at inoculation only. Inset: corresponding growth curve showing the onset stationary phase and timing of 2nd nitrogen addition; n=3 independent cultures, average of 281 cells counted per replicate, data are mean values, error bars are s.d..

160 Cells differentiated into oogonia and auxospores regardless of whether ammonium was
161 supplied at inoculation or at the onset of stationary phase (Fig. 1B). Thus, it appears that
162 stationary phase and ammonium availability are key factors that trigger formation of sexual cells
163 in centric diatoms. Resource depletion can arrest the cell cycle [14], and the presence of
164 ammonium at the onset of stationary phase appears to activate the sexual cycle. Auxospore
165 formation was observed in *Cyclotella meneghiniana* during stationary phase [28], and other
166 protists initiate sex under stress in response to nutrient depletion or oxidative DNA damage [29].
167 Ammonium can inhibit photosynthesis [27]; however, diatoms, including *T. pseudonana*, can
168 acclimate to millimolar ammonium concentrations [30]. It is possible that high ammonium
169 concentrations intensify the stress condition required for the sexual pathway. Nevertheless,
170 ammonium consistently caused formation of ten-fold more sexualized cells than the same
171 concentrations of nitrate (Fig 2 and S1).
172 Our results showing that ammonium induced formation of sexual cells in several centric
173 diatom species suggests that it may serve as a key environmental factor regulating the sexual
174 lifecycle across centric diatoms. Ammonium is typically present in very low concentrations in
175 aquatic ecosystems. However, ammonium reached 12.6 mM in a eutrophic lake where the centric
176 diatom, *Aulacoseira subarctica,* was observed undergoing sexual reproduction [8]. Clearly,
177 ammonium was not the growth-limiting nutrient under those conditions or in our laboratory
178 cultures (Fig 2). *Pseudo-nitzschia* auxospore formation was positively correlated with
179 ammonium, which was measured to be 14 μM during a major bloom event off the coast of
180 Washington [7]. Thus, the formation of sexual cells appears to be triggered by the presence of
181 ammonium while at least one other growth factor becomes limiting, such as light (discussed
182 below), phosphorous, silica [7], vitamins, or trace elements.

183 Cell differentiation in *T. pseudonana* was induced irrespective of growth rate in
184 exponential phase, light intensity, or light regime. However, the growth parameters did affect the
185 proportion of differentiated cells. Oogonia and auxospores were only 0.5% of the population
186 when grown under very low light (5 μE) with 200 μM NH_4Cl and increased to 39% when grown
187 under moderate light (100 μE) and 800 μM NH_4Cl (Table 1). The proportions of oogonia and
188 auxospores increased with light up to moderate intensities (70-100 μE) but decreased at high
189 (220 μE) intensities (Table 1), suggesting that photon flux has an important role in meeting the
190 energetic demands of sexual reproduction. Other work showed sexualization was more prevalent
191 at light <50 μE [31] or with the addition of a dark period [13, 32, 33]. Likely, the optimum light
192 intensity or need for a dark period to precede sexual induction [34] is species-specific and linked
193 to adaptive life histories [5].

194

195 **Table 1.** Effects of growth parameters on induction of sexual reproduction in *T. pseudonana*
196 CCMP1335, *T. weissflogii* and *C. cryptica*. Oogonia and auxospores always appeared in
197 stationary phase. The percentage of the total population (at least 300 cells counted per replicate)
198 differentiated into oogonia or auxospores when grown in nitrate or ammonium is shown for the
199 day they were at their maximum number; data are mean values ± s.d., biological replicates n=3.

Species	Light intensity (μE)	Light regime	Nitrogen concentration (μM)	Specific growth rate (d^{-1})	Oogonia and auxospores in NO_3^- (%)	Oogonia and auxospores in NH_4^+ (%)
T. pseudonana	5	24 h	200	0.28	0.21 ± 0.22	0.52 ± 0.52
	50	24 h	200	0.89	3.67 ± 0.55	7.67 ± 0.50
	50	12 h/12 h L/D	200	0.80	0.67 ± 0.27	2.32 ± 0.52
	220	24 h	200	1.2	0.26 ± 0.26	1.30 ± 0.91
	70	24 h	800	0.98	3.01 ± 0.52	38.9 ± 0.04

C. cryptica	100	24 h	800	0.38	11.1 ± 2.27	37.6 ± 3.71
T. weissflogii	100	24 h	800	0.52	4.50 ± 2.36	39.8 ± 5.65

200

201

202 ## Visualization of sexual morphologies

203 Confocal, light, and scanning electron microscopy were used to document the cell
204 morphologies at various stages in the life history cycle of *T. pseudonana* (Fig 3 and S2). Oogonia
205 were elongated relative to asexually growing vegetative cells and exhibited a bent morphology
206 and swelling of the plasma membrane at the junction of the hypotheca and epitheca (Figs 3B, 3C
207 and S2B-D). In oogonia, cellular contents became localized to the ends of the cell resulting in an
208 apparent empty space near the area of membrane swelling where fertilization likely occurs [5].

209

210

211 **Fig 3. The life cycle stages of *T. pseudonana* (A-K), T. weissflogii (L) and C. cryptica (M-O)**
212 **imaged using scanning electron microscopy (SEM), light (LM), and confocal microscopy**
213 **(CFM). A:** Two vegetative cells (LM, CCMP1335). **B:** Oogonium displaying separation of
214 thecae (arrowhead) and putative pycnotic nucleus indicated by the arrow (CFM, CCMP1015). **C:**
215 Oogonium sharply bending at the thecae junction. Arrowhead indicates protrusion of the plasma
216 membrane (CFM, CCMP1335). Oogonia images are representative of 38 total images. **D:**
217 Spermatogonium containing multiple spermatocytes seen as individual red (DNA stained)
218 clusters (CFM, CCMP1335); representative of 8 images. **E:** Motile spermatocytes (in red, arrow)
219 with moving flagella (arrowheads, CFM, CCMP1335, representative of 10 images). **F-G:** SEM
220 images of spermatocytes (arrowhead) attached to early oogonia (SEM, CCMP1335,
221 representative of 20 images). **H,I:** Auxospores; representative of 60 images in CCMP1015 (H,

222 LM) and CCMP1335 (I, CFM) showing bulging where mother valve was attached (arrowhead).
223 Two nuclei are visible in red following non-cytokinetic mitosis. **J:** Small parental cell (arrow)
224 with initial cells produced by sexual reproduction to the left (partial valve view) and right (girdle
225 view) indicated by the arrowheads (SEM, CCMP1335). **K:** 7 x 12 µm initial cell (LM); j and k
226 representative of 12 images of CCMP1335. **L:** *T. weissflogii* auxospore (LM); representative of
227 12 similar images. **M:** *C. cryptica* spermatogonium (upper left) and vegetative cell (lower right).
228 CFM shows stained DNA (red, arrow) and multiple nuclei in the spermatogonium. Arrowheads
229 indicate chlorophyll autofluorescence (green). Oogonium (**N**, representative of 6 images) and
230 auxospore (**O**, representative of 4 similar images) of *C. cryptica* (LM). Confocal microscopy
231 images (b-e, i, m) show chlorophyll autofluorescence (green) and Hoescht 33342 stained DNA
232 (red). Scale bars: **A**: 5 µm; **B-E**: 5 µm; **F**: 2 µm; **G**: 1 µm; **H-O**: 10 µm.
233
234
235 *T. pseudonana* spermatogonium harbored at least eight nuclei (Fig 3D), suggesting that a
236 depauperating mitosis preceded meiosis [11, 35]. Sperm released were very small, about 1 µm,
237 and flagellated (Figs 3E and S2E, S2F), but they often became entangled with other cells and
238 debris [8, 36, 37]. Sperm cells attached to oogonia at the junction of the thecae for fertilization
239 (Figs 3F, 3G and S2I, S2J) as shown in *T. punctigera* [38]. Also similar to *T. punctigera*, flagella
240 were not visible at that stage, possibly because flagella are abandoned upon attachment to the
241 oogonia [36].
242 Oogonia developed into auxospores and these conspicuous cell morphologies were
243 always observed in cultures induced by ammonium. Auxospores were larger than vegetative
244 cells and oogonia, ranging from about 6 to 20 µm in diameter, with most being 10-15 µm in

245 diameter (Figs 3H, 3I and S2G, S2H, S2L). Auxospores were spherical, with most of the cellular
246 contents localized to one side (Fig 3H, 3I and S2G, S2H, S2L) and sometimes showing slight
247 distention where the mother valve was shed (Fig 3I), as described in *Stephanodiscus niagarae*
248 [39]. Thecae remained attached in some cases, especially on smaller cells. Oogonia, auxospores,
249 and spermatogonia in the other species studied displayed similar morphologies to those observed
250 in *T. pseudonana* and other centric diatoms (Figs 3L-O, S2M-P and 4A) [11, 16, 28, 33, 35, 37,
251 38, 40, 41].
252
253
254 **Fig 4. Evidence for meiosis and initial cells**. **A:** 18s rRNA phylogeny of diatoms including
255 pennates (pink rectangle), centrics (blue rectangle). Highlighted in red are the four strains
256 induced into sexual reproduction in this study. Species for which some evidence already exists
257 for sexual reproduction are starred [9, 13, 16, 28, 33, 38]. **B-D:** Changes in DNA and chlorophyll
258 fluorescence in exponential (EXP), stationary (STA) and late stationary (L-STA) growth phases
259 of *T. pseudonana* induced by ammonium; 30,000 events recorded, representative of two
260 biological replicates. **E:** Coulter Counter distributions of cell diameter for *T. pseudonana*
261 cultures in exponential phase of growth and maintained in $NaNO_3$ (red) and after six successive
262 25% transfers to medium with ammonium (blue). Each new culture was allowed to remain in
263 stationary phase for three days before the next 25% transfer was made. Single replicates of
264 cultures with cell densities of 2.4×10^6 ml^{-1} ($NaNO_3$) and 2.3×10^6 ml^{-1} (ammonium). Dashed
265 lines are the mode for each peak.
266
267

268 Changes in DNA content in *T. pseudonana* cells induced into sexuality by ammonium
269 were observed using flow cytometry-based analysis. Fluorescence-activated cell sorting (FACS)
270 analysis showed that as the culture progressed from exponential into stationary growth phases,
271 the diploid population (Fig 4B) expanded to include DNA fluorescence intensities that were
272 consistent with the presence of spermatogonangia and spermatogonia containing multiple
273 gametes (Fig 4C). In late stationary phase, a new population was observed that had DNA
274 fluorescence signals consistent with haploid sperm cells with little to no chlorophyll [13] (Fig
275 4D).
276 Cell size restitution via auxosporulation produced progeny cells that were considerably
277 larger than the parent cells from nitrate stock cultures. To induce a high proportion of the eligible
278 cells into the sexual pathway we repeatedly propagated cultures in 800 µM ammonium with
279 inoculum of 25%. This strategy raises the ratio between the exposure of cells to ammonium in
280 stationary phase and the total number of cell divisions. Our findings can be explained by
281 assuming that cells in nitrate stock cultures are already at or below the critical size threshold for
282 induction into sexuality, but with each passage through growth and stationary phases in batch
283 culture, only a fraction of the eligible cells are induced into the sexual cycle. The average cell
284 diameters of the resulting cultures were larger relative to stock cultures maintained in nitrate (Fig
285 4E and S3). The *T. pseudonana* initial cells were 7-12 µm, the largest size reported for this
286 species (Figs 3J, 3K, S2K). Presuming that cell size reduction during vegetative growth occurs in
287 *T. pseudonana,* this process of cell size reduction and cell size restitution via ammonium
288 induction have opposing influences on the average size of populations. These processes
289 confound the ability to observe the impacts of sexual induction without experimental designs that

290 maximize the percentage of the population induced into the sexual pathway and minimize the
291 number of vegetative replications between episodes of induction.
292 We identified oogonia, male gametes, auxospores, and initial cells in cultures of the
293 model centric diatom, *T. pseudonana* providing new evidence for sexuality in this species that
294 was previously assumed to be asexual [10]. Although cell enlargement through
295 asexual/apomictic mechanisms has been recorded in other species [42-44], the presence of all
296 sexual cell types, and the expression of meiotic genes (discussed below), suggest apomixis is not
297 the mechanism being used by *T. pseudonana* for cell enlargement. Furthermore, apomixis
298 typically occurs in species that also undergo sexual reproduction [5]. Only spermatogenesis had
299 previously been reported in *T. weissflogii* [13, 45], but we have now also documented induction
300 of oogonia and auxospores by ammonium and subsequent formation of initial cells in this
301 species. A major challenge in visualizing the morphological characteristics of these species is
302 their smaller cell sizes compared to other species for which morphological details have been
303 documented. Now that we have determined a reliable method for inducing the sexual
304 morphologies, future studies will dissect additional details associated with the sexual pathways
305 in these, and perhaps other species inducible by ammonium, to determine their variation from
306 other centric diatoms. For example, the presence of auxospore scales, precise timing of
307 fertilization and meiotic activity, repeated auxosporulation, and polyspermy events (e.g., [38]).
308 The case of *T. pseudonana* also presents interesting questions about whether this species has
309 retained the ability to reduce in cell size. It appears that *T. pseudonana* has the capacity to avoid
310 clonal death by maintaining a relatively constant cell size (3-9 μM) [46-48]. Our experiments
311 show that cells in this size range are inducible into the sexual pathway. Nevertheless, the

312 question remains whether the progeny of induced small cells of *T. pseudonana* are capable of
313 cell size reduction.
314

315 Gene expression analysis of ammonium induced sexual
316 morphologies

317 We used RNAseq to identify genes that were differentially expressed in conditions that
318 triggered cell differentiation into sexual morphologies. We compared the transcriptomes of *T.*
319 *pseudonana* harvested in exponential (EXP), stationary (STA), and late stationary phases (L-
320 STA). Cells were grown in 100 μM $NaNO_3$ or, to capture a dose-dependent change in gene
321 expression, either 100 or 800 μM NH_4Cl (S4 Fig). We identified genes that were significantly
322 differentially expressed in multiple pairwise comparisons of growth phases and nitrogen sources
323 (S1-S11 Tables). Next, we examined the statistical interactions of pairwise condition
324 comparisons to identify genes with significantly greater or lesser magnitude changes in
325 expression between growth stages in the presence of ammonium relative to 100 μM $NaNO_3$ (Fig
326 5A and S5).
327
328
329 **Fig 5. Transcriptomic evidence for sexual reproduction in *T. pseudonana*. A:** Heat map of 89
330 genes having annotated functions that were differentially expressed during differentiation and
331 sexual reproduction in *T. pseudonana* CCMP1335. Color indicates normalized expression value
332 (FPKM) for each nitrogen treatment (control = 100 μM NO_3^-; 100NH4 = 100 μM NH_4^+;
333 800NH4 = 800 μM NH_4^+) and growth phase (EXP, STA, L-STA). **B:** FPKM values of select
334 genes across growth phases for each nitrogen treatment.

335

336

337 This conservative approach yielded a total of 1,274 genes in the four analyses of
338 statistical interactions (S12-S15 Tables). A total of 89 of the genes have an annotated function
339 (Fig. 5A;S16 Table). The set of 89 genes includes four meiotic genes (*mcm2, mcm8, mcm9, and*
340 *mlh1*, Fig 4B and S6) that were also up-regulated in pennate diatoms during sexual reproduction
341 [26]. The Mcm family of DNA helicases function in DNA replication, with *mcm8, mcm9,* and
342 *mlh1* having roles in double stranded break repair [49-51]. Mcm8 was one of the four genes
343 related to meiosis that were upregulated in the pennate diatom, *Seminavis robusta* during
344 treatment with a sex-inducing pheromone [17]. Eight genes in our list are homologous to yeast
345 genes involved in meiosis [52] (Fig 5B,S17 Table), including genes that regulate the meiotic
346 anaphase promoting complex (*cdc16*, *cdc23*, *ama1*) [53, 54] and *rad54*, a motor protein that
347 regulates branch migration of Holliday junctions during homologous recombination [55].
348 Expression of genes encoding other RAD proteins (*rad50 and rad 51*) increased in pennate
349 diatoms induced into meiosis [17, 26].

350 Of three 'sexually induced genes' that were up-regulated in *T. weissflogii* at the initiation
351 of gametogenesis [45] and associated with sperm flagella mastigonemes [56], one, *sig3*, was
352 significantly up-regulated in stationary phase compared to exponential phase (Fig 5B). In
353 addition, a gene encoding an intraflagellar transport protein (IFT88) was also up-regulated in
354 ammonium induced cells during stationary phase (Fig. 5B). An IFT system is required for
355 flagellar assembly [57] and five genes encoding IFT particle proteins, including IFT88, and a
356 kinesin-associated protein involved in anterograde transport were found in the *T. pseudonana*
357 genome [58]. The genes encoding Sig3 and IFT88 are unique to flagellar structures, and their

358 differential expression in ammonium induced *T. pseudonana* compared to the nitrate-grown
359 control treatments provide additional evidence that ammonium induced spermatogenesis in this
360 species.

361 The MYB factor and bZIP families of proteins are transcriptional regulators that control a
362 variety of cell processes including stress responses, development, and differentiation in plants
363 [59]. Expression of two genes having the characteristic R2R3 MYB DNA binding domains
364 common in plants, *myb24 and myb16,* was generally lower in ammonium induced cultures
365 compared to the nitrate grown controls (Fig 5B). In *Arabidopsis thaliana*, hormonal activation of
366 *myb24* is required for stamen development and male fertility [60]. Whether *myb24, myb16,* and
367 *bzip2* play roles in regulating gamete development or sex differentiation in diatoms remains to be
368 determined.

369 The 1,274 genes provide new avenues to understand the evolution of sexuality in the
370 Heterokont eukaryotic lineage. Diatoms emerged ~ 200 Mya, about 800 My after a eukaryotic
371 heterotroph engulfed a red alga in the secondary endosymbiosis event that gave rise to the SAR
372 eukaryotic supergroup [61]. Of 171 diatom genes of red algal origin [61], 17 were identified as
373 differentially expressed in conditions that induced sexual reproduction (S18 Table). None of
374 these genes are annotated in the *T. pseudonana* genome, but in red algae they are predicted to
375 function in transport and plastid-targeted processes [23].

376

377 # Conclusions

378 That some of the most well studied centric diatoms were never observed undergoing
379 sexual reproduction was a mystery. Possibly even more elusive was the ability to reliably control
380 or induce the sexual pathway of centric diatoms in the laboratory [10] despite a myriad of efforts

381 that ranged from sweet-talk to torture. Factors that have limited progress in this field center on
382 the problem that even under 'favorable environmental conditions' that result in the sexual
383 lifecycle, only a fraction of cells undergo sexual reproduction (Fig 2). Thus, capturing the sexual
384 event requires near constant visual observation because (a) only cells that have become
385 sufficiently small and reach the critical size threshold can undergo sexual reproduction [62], (b)
386 only a fraction of those size-eligible cells may undergo sexual reproduction [8, 15, 16, 31], (c)
387 there has been a lack of understanding about what constitutes conditions that are 'favorable' for
388 triggering diatom sex [5, 7], and (d) morphological changes indicative of sex may not be
389 recognized by untrained scientists [63].

390 Our results provide strong evidence that *T. pseudonana* is a sexual organism, expressing
391 the major morphologies associated with the sexual pathway that result in enlarged initial cells.
392 Furthermore, the sexual pathway was reliably induced in *T. pseudonana*, and two other centric
393 diatom species by exposure of size-eligible cells to ammonium. Ammonium triggered formation
394 of sexual cells in a dose-dependent manner and significant changes in expression of genes
395 involved in meiosis, spermatocyte flagellar structures and assembly, and sex differentiation.
396 RNAseq analysis revealed many more genes with unknown functions that were expressed under
397 conditions of sexual differentiation. Other genes involved in sex are likely to have been missed
398 by our analysis because their changes in expression were masked by the mixed population of
399 asexual and sexual cells, or they were not captured in the coarse time-resolution of sampling
400 used in this study. Nevertheless, our discoveries resolve two persistent mysteries that have
401 plagued diatom researchers. Furthermore, the RNAseq data provide a subset of genes that can be
402 used to study the molecular ecology of diatoms.

The ecology of centric diatom sexual reproduction that can be inferred from our findings appears best described as synchronous sexuality [12] triggered by ammonium in cells experiencing growth stress. Asexual cell cycle arrest appears to be prerequisite to activation of the diatom sexual life cycle [13, 14, 28, 29]. In the environment, diatoms bloom following elevated nutrient concentrations driven by vertical mixing, coastal upwelling, or river inputs and the bloom reaches its peak biomass when essential nutrients are depleted. Within a week, the bulk of a bloom can be consumed by heterotrophic protists [64] that excrete ammonium to maintain homeostatic elemental composition [65]. We propose that ammonium released by grazers at bloom climax may be a principal ecological trigger for sexual morphologies in centric diatoms. Synchronization of sexuality at the onset of resource depletion (stationary phase) increases the chances for successful fertilization because cell density is at its maximum [12]. Environmental concentrations of ammonium in the environment rarely reach the concentrations used in this study to demonstrate the dose response effect on sexuality. Other methods that have sometimes successfully triggered sexual reproduction in other species are similarly unusual compared to environmental conditions. For example, the magnitude of the salinity shifts used to induce sexual reproduction in *Skeletonema marioni* in the laboratory do not occur in the Baltic sea [16]. Nevertheless, pulses of ammonium, shifts in salinity, and other environmental fluctuations do occur in aquatic ecosystems, and provided the other conditions for sexuality are met (e.g., cell size threshold, stress, population density), are likely to induce sexuality in at least a small fraction of a population. The presence of ammonium and the onset of stationary phase also point to involvement of another growth factor whose depletion triggers sexual reproduction. The specific collection of factors that lead to sexual reproduction in diatoms in the environment is not yet known and neither is whether ammonium is a direct or indirect trigger of sexuality [4].

426 Nevertheless, this work suggests an intriguing ecological role for ammonium in the mechanisms
427 underlying sexuality in centric diatoms and will certainly be a valuable tool to control sexuality
428 in the laboratory.

429 The identification of ammonium as a reliable inducer of sexuality in *T. pseudonana* and
430 other centric diatoms has the potential to shift perspectives on diatom ecology, open avenues for
431 the experimental investigation of diatom reproductive mechanisms, and provide tools for genetic
432 manipulation of centric diatoms that have not heretofore been available. Diatom blooms have a
433 global impact but the factors that control these blooms and their demise are complex and a
434 consensus has not been reached about these processes. Our evidence suggests that induction of
435 sexuality may play a vital role in diatom bloom conclusion and the production of genetic
436 diversity that seeds future blooms [66]. Our analysis suggests an involvement of genes of red-
437 algal origin, providing new lines of evolutionary enquiry. Interest in diatoms for biotechnological
438 applications is high due to their uses in biofuels, materials chemistry and medicine. Our work
439 will likely propel this exploration by enabling improved breeding and genetic modification to
440 control and understand unique diatom traits.
441

442 Materials and methods

443 Stock cultures of *T. pseudonana* (CCMP1335) were maintained in f/2 medium [67] with
444 200 μM $NaNO_3$ under continuous sub-saturating light at 18°C. Sexual cells were quantified in
445 triplicate cultures of *T. pseudonana* (CCMP1335 and CCMP1015), *T. weissflogii* (CCMP1336)
446 and *C. cryptica* (CCMP332) (all obtained from NCMA) grown in f/2 amended with $NaNO_3$ or
447 NH_4Cl and grown at 18°C under 50 μE continuous light, or under variable light intensities/cycles

448 as shown in Table 1. Cell populations were quantified using a Coulter counter (Beckman-
449 Coulter, Indianapolis, Indiana). Oogonia and auxospores were counted using a hemocytometer.
450 We found that a modified f/2 medium yielded better cell images using light and confocal
451 microscopy. This medium contained 0.939 mM KCl, 0.802 mM NO_3^-, 1 mM NH_4Cl, 0.05 mM
452 glycine, 0.01 mM methionine, 0.078 mM pyruvate, 0.84 μM pantothenate, 0.985 μM 4-amino-5-
453 hydroxymethyl-2-methylpyrimidine, 0.3 μM thiamine, 0.002 μM biotin, 0.117 μM $FeCl_3*6H_2O$,
454 0.009 μM $MnCl_2*4H_2O$, 0.0008 μM $ZnSO_4*7H_2O$, 0.0005 μM $CoCl_2*6H_2O$, 0.0003 μM
455 $Na_2MoO_4*2H_2O$, 0.001 μM Na_2SeO_3, and 0.001 μM $NiCl_2*6H_2O$, and sparged with filter-
456 sterilized carbon dioxide and air for 8 hours and overnight respectively. To view DNA, 1 ml live
457 samples were stained with 5 μl 1.62 μM Hoescht 33342 (0.2 μm filtered) for 10 min. For
458 scanning electron microscopy (SEM), 1 ml samples were diluted 1:3 with sterile f/2 and syringe
459 filtered onto 13 mm 0.2 μm polycarbonate filters using a Swinnex filter unit. The filter was
460 washed with 4 ml f/2 containing 0.5% gluteraldehyde and left submerged for at least 24 hours,
461 followed by a series of 4 ml washes: 0.2 μm filtered 80%, 60%, 40%, 20% and 0% f/2, followed
462 by 20%, 40%, 60% 80% and 100% ethanol, before critical point drying. SEM imaging was done
463 at the Oregon State University Electron Microscope facility.
464 For flow cytometry 1 ml culture samples were fixed with 1 μl gluteraldehyde (50%) and
465 stained with 10 μl Sybr green mix (1:25 dilution Sybr green in 0.01M Tris-EDTA, pH 8.0) for 30
466 min. Samples were run on a FACScan flow cytometer (Becton Dickinson, Franklin Lakes, New
467 Jersey). Settings were FL1=582 and FL3=450 for unstained cells and FL1=450 and FL3=450 for
468 stained cells.
469 For RNAseq analysis, $1.61x10^8$ – $1.10x10^9$ cells from triplicate independent cultures
470 were filtered onto 0.8 μm 47 mm polycarbonate filters during exponential, stationary and late

471 stationary phases and flash frozen in liquid nitrogen. RNA was extracted using a Qiagen RNeasy
472 midi kit according to modified manufacturer's instructions [68]. Silica beads (0.5 mm) were
473 added to the cells and lysis buffer and vortexed until homogeneous before being filtered through
474 Qiashredder columns to remove large particles. Eluted RNA was subjected to off column RNase
475 free DNase I treatment and secondary purification according to manufacturer's
476 recommendations. Total RNA was prepared and sequenced as a 150 bp single end library on an
477 Illumina HiSeq 3000 at the Center for Genome Research and Biocomputing at Oregon State
478 University. Sequencing data/interaction analyses were conducted using the Ballgown pipeline
479 [69]. Sequencing reads were trimmed to remove sequencing adapters using BBDuk v. with the
480 parameters " ktrim=r k=23 mink=9 hdist=1 minlength=100 tpe tbo" [70]. Reads aligned to the *T.*
481 *pseudonana* reference genome (NCBI accession GCA_000149405.2) using HISAT2 v. 2.0.4
482 with the parameters " --min-intronlen 20 --max-intronlen 1500 --rna-strandness F --dta-cufflinks"
483 [71]. Transcripts were assembled for each dataset and merged using Stringtie v 1.2.4 [72].
484 Pairwise differential expression analyses for genes were performed using the "stattest" function
485 in Ballgown version 2.2.0 [73]. Interaction effects were tested by comparing the models with
486 (timepoint + treatment + timepoint * treatment) and without (timepoint + treatment) the
487 interaction term using the custom model option in the "stattest" function.
488 For construction of the phylogenetic tree, 18s rRNA sequences were obtained from the
489 Silva database and aligned using Muscle v3.8.31 (default settings) [74]. A genome editor
490 (BioEdit) was used to manually trim off overhanging sequence. The tree was built using
491 RAxML-HPC v8.0.26 using the GTRCAT model, "-f a" option, and 1000 bootstrap replicates
492 [75]. A visual representation was created using the TreeDyn [76] tool through LIRMM
493 (phylogeny.fr) [77].

494 All RNAseq data have been deposited to NCBI under BioProject ID PRJNA391000.

495

496 # Acknowledgements

497 The authors thank Kelsey McBeain for assistance with confocal microscopy imaging and the

498 Electron Microscope Facility at Oregon State University for scanning electron micrographs.

499

References

1. Nelson DM, Tréguer P, Brzezinski MA, Leynaert A, Quéguiner B. Production and dissolution of biogenic silica in the ocean: Revised global estimates, comparison with regional data and relationship to biogenic sedimentation Biogeochem Cycles. 1995;9(3):359-72.
2. Mann DG. The species concept in diatoms. Phycologia. 1999;38:437-95.
3. Simonsen R. The diatom system: Ideas on phylogeny. Bacillaria. 1979;2:9-71.
4. Lewis WM. The diatom sex clock and its evolutionary importance. Amer Naturalist. 1984;123:73-80.
5. Chepurnov VA, Mann DG, Sabbe K, Vyverman W. Experimental studies on sexual reproduction in diatoms. In: Jeon KW, editor. A Survey of Cell Biology. International Review of Cytology. 237. London, UK: Elsevier Academic Press; 2004. p. 91-154.
6. Drebes. Sexuality. In: Werner D, editor. The Biology of Diatoms. Botanical Monographs. 13. Oxford: Blackwell Scientific Publications; 1977. p. 250-83.
7. Holtermann KE, Bates SS, Trainer VL, Odell A, Armbrust EV. Mass sexual reproduction in the toxigenic diatoms *Pseudo-Nitzscia australis* and *P. pungens* (Bacillariophyceaea) on the Washington coast, USA. J Phycol. 2010;46:41-52. doi: 10.1111/j.1529-8817.2009.00792.x.
8. Jewson DH. Size reduction, reproductive strategy and the life cycle of a centric diatom. Philos T R Soc B. 1992;336:191-213.
9. Koester JA, Brawley SH, Karp-Boss L, Mann DG. Sexual reproduction in the marine centric diatom *Ditylum brightwellii* (Bacillariophyta). Eur J Phycol. 2008;42(4):351-66.

10. Chepurnov VA, Mann DG, von Dassow P, Vanormelingen P, Gillard J, Inze D, et al. In search of new tractable diatoms for experimental biology. BioEssays. 2008;30:692-702.

11. Von Dassow P, Montresor M. Unveiling the mysteries of phytoplankton life cycles: patterns and opportunities behind complexity. J Plankton Res. 2011;33(1):3-12.

12. Edlund MB, Stoermer EF. Ecological, evolutionary, and systematic significance of diatom life histories. J Phycol. 1997;33:897-918.

13. Armbrust EV, Chisholm SW, Olson RJ. Role of light and the cell cycle on the induction of spermatogenesis in a centric diatom. J Phycol. 1990;26(3):470-8. doi: 10.1111/j.0022-3646.1990.00470.x.

14. Huysman MJJ, Vyverman W, De Veylder L. Molecular regulation of the diatom cell cycle. J Exp Bot. 2014;65(10):2573-84.

15. Assmy P, Henjes J, Smetacek V, Montresor M. Auxospore formation in the silica-sinking oceanic diatom *Fragilariopsis kerguelensis* (Bacillariophyceae). J Phycol. 2006;42:1002-6.

16. Godhe A, Kremp A, Montresor M. Genetic and microscopic evidence for sexual reproduction in the centric diatom *Skeletonema marinoi*. Protist. 2014;165(4):401-16. doi: 10.1046/j.protis.2014.04.006.

17. Moeys S, Frenkel J, Lembke C, Gillard JTF, Devos V, Van den Berge K, et al. A sex-inducing pheromone triggers cell cycle arrest and mate attraction in the diatom Seminavis robusta. Sci Reports. 2016;6:19252. doi: 10.1038/srep19252.

18. Ezzati J, Dolatabadi N, de la Guardia M. Applications of diatoms and silica nanotechnology in biosensing, drug and gene delivery, and formation of complex metal nanostructures. J Analyt Chem. 2011;30(9):1538-48.

19. Kroth P. Molecular biology and the biotechnological potential of diatoms. Adv Exp Med Biol. 2007;616:23-33.

20. d'Ippolito G, Sardo A, Paris D, Vella FM, Adelfi MG, Botte P, et al. Potential of lipid metabolism in marine diatoms for biofuel production. Biotechnology for Biofuels. 2015;8:28-38. doi: 10.1186/s13068-015-0212-4.

21. Hildebrand D, Smith SR, Traller JC, Abbriano RM. The place of diatoms in the biofuels industry. Biofuels. 2012;3(2):221-40.

22. Armbrust EV, Berges JA, Bowler C, Green BR, Martinez D, Putnam NH, et al. The genome of the diatom *Thalassiosira pseudonana*: Ecology, evolution, and metabolism. Science. 2004;306:79-86.

23. Bowler CB, Allen AE, Badger JH, Grimwood J, Jabbari K, Kuo A, et al. The *Phaeodactylum* genome reveals the evolutionary history of diatom genomes. Nature. 2008;456(7219):239-44.

24. Chepurnov VA, Chaerle P, Roef L, Van Meirhaeghe A, Vanhoutte K. Classical breeding in diatoms: Scientific background and practical perspectives. Diatom Biology. Cellular Origin, Life in Extreme Habitats and Astrobiology. 19: Springer; 2011. p. 167-94.

25. Apt KE, Kroth-Pancic PG, Grossman A. Stable nuclear transformation of the diatom *Phaeodactylum tricornutum*. Mol Gen Genet. 1996;252(5):572-9.

26. Patil S, Moeys S, Von Dassow P, Huysman MJJ, Mapleson D, De Veylder L, et al. Identification of the meitic toolkit in diatoms and exploration of meiosis-specific *SPO11* and *RAD51* homologs in the sexual species *Pseudo-nitzchia multistriata* and *Seminavis robusta*. BMC Genomics. 2015;2015(930). doi: 10.1186/s12864-015-1983-5.

27. Yoshiyama K, Sharp JH. Phytoplankton response to nutrient enrichment in an urbanized estuary: Apparent inhibition of primary production by overeutrophication. Limnol Oceanogr. 2006;51(1, part 2):424-34.

28. Hoops HJ, Floyd GL. Ultrastructure of the centric diatom, *Cyclotella meneghiniana*: vegetative cell and auxospore development. Phycologia. 1979;18:424-35.

29. Bernstein H, Bernstein C. Evolutionary origin of recombination during meiosis. BioScience. 2010;60(7):498-505. doi: 10.1525/bio.2010.60.7.5.

30. Collos Y, Harrison PJ. Acclimation and toxicity of high ammonium concentrations to unicellular alage. Mar Poll Bull. 2014;80(1-2):8-23. doi: 10.1016/j.marpolbul.2014.01.006.

31. Mouget J-L, Gastineau R, Davidovich O, Gaudin P, Davidovich NA. Light is a key factor in triggering sexual reproduction in the pennate diatom *Haslea ostrearia*. FEMS Microbiol Ecol. 2009;69(2):194-201.

32. Vaulot D, Chisholm SW. A simple model for the growth of phytoplankton populations in light/dark cycles. J Plankton Res. 1987;9:345-66.

33. Mills KE, Kaczmarska I. Autogamic reproductive behavior and sex cell structure in *Thalassiosira angulata* (Bacillariophyta). Botanica Mar. 2006;49:417-30. doi: 10.1515/BOT.2006.053.

34. Gillard J, Devos V, Huysman MJJ, De Veylder L, D'Hondt S, Martens C, et al. Physiological and transcriptomic evidence for a close coupling between chloroplast ontogeny and cell cycle progression in the pennate diatom *Seminavis robusta*. Plant Physiol. 2008;148:1394-411. doi: 10.1104/pp.108.122176.

35. Kaczmarska I, Poulíčková A, Sato S, Edlund MB, Idei M, Watanabe T, et al. Proposals for a terminology for diatom sexual reproduction, auxospores and resting stages. J Diatom Res. 2013;28(3):263-94.

36. French III FW, Hargraves PE. Spore formation in the life cycles of the diatoms *Chaetoceros diadema* and *Leptocylindrus danicus*. J Phycol. 1985;21:477-83.

37. Idei M, Osada K, Sato S, Toyoda K, Nagumo T, Mann DG. Gametogenesis and auxospore development in *Actinocyclus* (Bacillariophyta). PLOS One. 2012;7(8):e41890.

38. Chepurnov VA, Mann DG, Von Dassow P, Armbrust EV, Sabbe K, Dasseville R, et al. Oogamous reproduction, with two-step auxosporulation, in the centric diatom *Thalassiosira punctigera* (Bacillariophyta). J Phycol. 2006;42:845-58. doi: 10.1111/j.1529-8817.2006.00244.x.

39. Edlund MB, Stoermer EF. Sexual reproduction in *Stephanodiscus niagarae* (Bacillariophyta). J Phycol. 1991;27:780-93.

40. Idei M, Sato S, Nagasato C, Motomura T, Toyoda K, Nagumo T, et al. Spermatogenesis and auxospore structure in the multipolar centric diatom Hydrosera. J Phycol. 2015;51(1):144-58.

41. Shirokawa Y, Shimada M. Sex allocation pattern of the diatom *Cyclotella meneghiniana*. Proceedings of the Royal Society B: Biological Sciences. 2013;280(1761):20130503.

42. Nagai S, Hori Y, Manabe T, Imai I. Restoration of cell size by vegetative cell enlargement in *Coscinodiscus wailesii* (Bacillariophyceae). Phycologia. 1995;34(6):533-5.

43. Sabbe K. Apomixis in *Achnanthes* (Bacillariophyceae); development of a model system for diatom reproductive biology. Eur J Phycol. 2004;39:327-41.

44. Gallagher JC. Cell Enlargement in *Skeletonema costatum* (Bacillariophyceae). J Phycol. 1983;19:539-42.

45. Armbrust EV. Identification of a new gene family expressed during the onset of sexual reproduction in the centric diatom *Thalassiosira weissflogii*. Appl Environ Micriobiol. 1999;65:3121-8.

46. Hildebrand M, Frigeri LG, Davis AK. Synchronized growth of *Thalassiosira pseudonana* (Bacillariophyceae) provides novel insights into cell-wall synthesis processes in relation to the cell cycle. J Phycol. 2007;43:730-40.

47. Hildebrand M, York E, Kelz JI, Davis AK, Frigeri LG, Allison DP, et al. Nanoscale control of silica morphology and three-dimensional structure during diatom cell wall formation. J Mater Res. 2006;21(10):2689-98.

48. Round FE. The problem of size reduction in diatoms. Nova Hedwig. 1972;23:291-303.

49. Lutzmann M, Grey C, Traver S, Ganier O, Maya-Mendoza A, Ranisavljevic N, et al. MCM8- and MCM9-deficient mice reveal gametogenesis defects and genome instability due to impaired homologous recombination. Mol Cell. 2012;47(4):523-34.

50. Park J, Long DT, Lee KY, Abbas T, Shibata E, Negishi M, et al. The MCM8-MCM9 complex promotes RAD51 recruitment at DNA damage sites to facilitate homologous recombination. Mol Cell Biol. 2013;33(8):1632-44.

51. Baker SM, Plug AW, Prolla TA, Bronner CE, Harris AC, Yao X, et al. Involvement of mouse Mlh1 in DNA mismatch repair and meiotic crossing over. Nat Genet. 1996;13(3):336-42.

52. Butler G, Rasmussen MD, Lin MF, Santos MAS, Sakthikumar S, Munro CA, et al. Evolution of pathogenicity and sexual reproduction in eight *Candida* genomes. Nature. 2009;459:657-62. doi: 10.1038/nature08064.

53. Cooper KF, Mallory JJ, Egeland DB, Jarnik M, Strich R. Ama1p is a meiosis-specific regulator of the anaphase promoting complex/cyclosome in yeast. PNAS. 2000;97(26):14548-53. doi: 10.1073/pnas.250351297.

54. Zachariae W, Shevchenko A, Andrews PD, Ciosk R, Galova M, Stark MJR, et al. Mass spectrometric analysis of the anaphase-promoting complex from yeast: Identificaiton of a subunit related to cullins. Science. 1998;279(5354):1216-9.

55. Mazin AV, Mazina OM, Bugreev DV, Rossi MJ. Rad54, the motor of homologous recombination. DNA Repair. 2010;9(3):286-302.

56. Honda D, Shono T, Kimura K, Fujita S, Iseki M, Makino Y, et al. Homologs of the sexually induced gene 1 (*sig1*) product constitute the Stramenopile mastigonemes. Protist. 2007;158(1):77-88.

57. Rosenbaum JL, Witman GB. Intraflagellar transport. Nat Rev Mol Cell Biol. 2002;3:813-25.

58. Merchant SS, Prochnik SE, Vallon O, Harris EH, Karpowicz SJ, Witman GB, et al. The *Chlamydomonas* genome reveals the evolution of key animal and plant functions. Science. 2007;318(5848):245-50. doi: 10.1126/science.1143609.

59. Ambawat S, Sharma P, Yadav NR, Yadav RC. MYB transcription factor genes as regulators for plant responses: an overview. Physiol Mol Biol Plants. 2013;19(3):307-21. doi: 10.1007/s12298-013-0179-1.

60. Cheng H, Song S, Xiao LX, Soo HM, cheng Z, Xie D, et al. Gibberellin acts through jasmonate to control the expression of *MYB21, MYB24,* and *MYB57* to promote stamen filament growth in *Arabidopsis*. Plos Genet. 2009;5. doi: 10.1371/journal.pgen.1000440.

61. Archibald JM. The puzzle of plastid evolution. Curr Biol. 2009;19(2):R81-R8.

62. Geitler L. Der Formwechsel der pennaten Diatomeen. Arch Protistenk. 1932;78(1):1-226.

63. Mann DG. Why didn't Lund see sex in Asterionella? A discussion of the diatom life cycle in nature. In: Round FE, editor. Algae and the Aquatic Environment, contributions in honour of JWG Lund. Bristol: Biopress; 1988. p. 384-412.

64. Tillmann U. Interactions between planktonic microalgae and protozoan grazers. J Euk Microbiol. 2004;51:156-68.

65. Sterner RW, Elser JJ. Ecological stoichiometry: the biology of elements from molecules to the biosphere. Princeton, New Jersey, USA: Princeton University Press; 2002.

66. Chen G, Rynearson TA. Genetically distinct populations of a diatom co-exist during the North Atlantic spring bloom. Limnol Oceanogr. 2016;61(6):2165-79. doi: 10.1002/lno.10361.

67. Guillard RRL. Culture of phytoplankton for feeding marine invertebrates. In: Smith WL, Chanley MH, editors. Culture of Marine Invertebrate Animals. New York: Plenum Press; 1975. p. 26-60.

68. Dyhrman ST, Jenkins BD, Rynearson TA, Saito MA, Mercier ML, Alexander H, et al. The transcriptome and proteome of the diatom *Thalassiosira pseudonana* reveal a diverse phosphorus stress response. PLOS One. 2012;7(3):e33768. doi: 10.1371/journal.pone.0033768.

69. Pertea M, Kim D, Pertea GM, Leek JT, Salzberg SL. Transcript-level expression analysis of RNA-seq experiments with HISAT, StringTie and Ballgown. Nat Prot. 2016;11:1650-67. doi: 10.1038/nprot.2016.095.

70. Bushnell B. BBtools 2016.

71. Kim D, Langmead B, Salzberg SL. HISAT: a fast spliced aligner with low memory requirements. Nat Methods. 2015;12:357-60.

72. Pertea M, Pertea GM, Antonescu CM, Chang TC, Mendell JT, Salzberg SL. StringTie enables improved reconstruction of a transcriptome from RNA-seq reads. Nat Biotech. 2015;33(290-295):290-5.

73. Frazee AC, Pertea GM, Jaffe AE, Langmead B, Salzberg SL, Leek JT. Ballgown bridges the gap between transcriptome assembly and expression analysis. Nat Biotech. 2015;33(3):243-6.

74. Edgar RC. MUSCLE: a multiple sequence alignment method with reduced time and space complexity. BMC Bioinformatics. 2004;19(5):113.

75. Stamatakis A. RAxML-VI-HPC: maximum likelihood-based phylogenetic analyses with thousands of taxa and mixed models. Bioinformatics. 2006;22:2688-90.

76. Chevenet F, Brun C, Bañuls AL, Jacq B, Christen R. TreeDyn: towards dynamic graphics and annotations for analyses of trees. BMC Bioinformatics. 2006;7:439.

77. Dereeper A, Guignon V, Blanc G, Audic S, Buffet S, Chevenet F, et al. Phylogeny.fr: robust phylogenetic analysis for the non-specialist. Nucleic Acids Res. 2008;1(36):W465-W9.

Supporting Information

S1 Fig. Ammonium induces sexual morphologies in *T. weissflogii* (A) and *C. cryptica* (B). Proportion of sexual cells (oogonia and auxospores) relative to the total population in cultures supplemented with NH_4Cl or $NaNO_3$. An average of 120 and 107 cells were counted per replicate of *T. weissflogii* and *C. cryptica*, respectively, throughout the growth curve, but oogonia and auxospores were only observed beginning in stationary phase; independent cultures n=3, data are mean values, error bars are s.d.. Inset: corresponding growth curve linking the onset of stationary phase with first appearance of sexual cells on day 10 (**A**) and 17 (**B**).

S2 Fig. The different life stages in *T. pseudonana* (A-L), *T. weissflogii* (M,N) and *C. cryptica* (O,P). A: SEM of vegetative cells (CCMP1335). **B-D:** SEM (B) and CFM images of CCMP1335 oogonia, displaying separation of the thecae and expansion of the membrane. **E:** CFM image of flagellated spermatocytes with stained DNA (arrowheads), **F, G**. Epifluorescence (F) and LM images of the same view. In F, an active, flagellated spermatocyte (arrowhead) possibly associated with an auxospore surface is revealed by lateral light from fluorescence of DNA (blue) and chlorophyll (red). **H,L:** Auxospores of CCMP1015 and CCMP1335 respectively (CFM). **I,J:** Individual spermatocytes attached to oogonia (SEM). **K:** Initial cells of *T. pseudonana* CCMP1335 (LM). **M,N:** *T. weissflogii* vegetative cells (M; LM) and auxospore (N; LM). **O,P:** *C. cryptica* oogonia (O; LM) and auxospores (P; LM). CFM images (C-E, H, L) show fluorescence of DNA in red and chlorophyll in green.

S3 Fig. Coulter Counter distributions of cell diameter for *T. weissflogii* (**A**) and *C. cryptica* (**B**) cultures in exponential phases of growth and maintained in $NaNO_3$ (red) and after two successive

24 25% transfers to media with ammonium (blue), Each new culture was allowed to remain in
25 stationary phase for three days before the next 25% transfer was made. Single replicates. Dashed
26 lines are the mode for each peak. Cell densities in (**A**) are 2.2 x 10^5 ml^{-1} ($NaNO_3$) and 3.3 x 10^5
27 ml^{-1} (ammonium) and (**B**) are 1.6 x 10^6 ml^{-1} ($NaNO_3$) and 2.2 x 10^6 ml^{-1} (ammonium).
28
29 **S4 Fig. *T. pseudonana* CCMP1335 growth and collection for RNAseq analysis.** Three
30 independent cultures of each nitrogen treatment were harvested 3, 5, and 8 days after inoculation
31 (down arrows) in exponential (EXP), stationary (STA) and late stationary phases (L-STA). The
32 100uM NH_4^+ STA treatment did not yield sufficient RNA for analysis.
33
34 **Table S1. Pairwise comparison, Stationary phase 800 µM Ammonium vs. exponential**
35 **phase 800 µM Ammonium.**
36
37 **Table S2. Pairwise comparison, Late-stationary phase 800 µM Ammonium vs. exponential**
38 **phase 800 µM Ammonium.**
39
40 **Table S3. Pairwise comparison, Exponential phase 100 µM Ammonium vs. Late stationary**
41 **phase 100 µM Ammonium.**
42
43 **Table S4. Pairwise comparison, Stationary phase 800 µM Ammonium vs. Late stationary**
44 **phase 800 µM Ammonium.**
45

Table S5. Pairwise comparison, Exponential phase nitrate vs. Exponential phase 800 µM Ammonium.

Table S6. Pairwise comparison, Stationary phase nitrate vs. Stationary phase 800 µM Ammonium.

Table S7. Pairwise comparison, Late Stationary phase nitrate vs. Late Stationary phase 800 µM Ammonium.

Table S8. Pairwise comparison, Exponential phase nitrate vs. Exponential phase 100 µM Ammonium.

Table S9. Pairwise comparison, Late Stationary phase nitrate vs. Late Stationary phase 100 µM Ammonium.

Table S10. Pairwise comparison, Exponential phase 100 µM Ammonium vs. Exponential phase 800 µM Ammonium.

Table S11. Pairwise comparison, Late Stationary phase 100 µM Ammonium vs. Late Stationary phase 800 µM Ammonium.

67 **S5 Fig. Interaction analysis workflow of RNAseq data.** Growth phase A vs. B is EXP vs.
68 STA, EXP vs. L-STA, or STA vs. L-STA, respectively. Δexp is the magnitude of change in gene
69 expression between growth phases for the different nitrogen treatments.
70
71 **Table S12. Interaction analysis, Exponential - Stationary phases (800 µM Ammonium v.**
72 **Nitrate control).**
73
74 **Table S13. Interaction analysis, Exponential - Late Stationary phases (800 µM Ammonium**
75 **v. Nitrate control).**
76
77 **Table S14. Interaction analysis, Exponential - Late Stationary phases (100 µM Ammonium**
78 **v. Nitrate control).**
79
80 **Table S15. Interaction analysis, Stationary - Late Stationary phases (800 µM Ammonium v.**
81 **Nitrate control).**
82
83 **Table S16. Genes that were identified as differentially expressed in conditions that**
84 **triggered cell differentiation and sexual reproduction and have annotated functions.**
85
86 **Table S17. Genes that were identified as differentially expressed in conditions that**
87 **triggered cell differentiation and sexual reproduction and are homologous to yeast genes**
88 **involved in meiosis.**
89

90 **Table S18. Genes that were identified as differentially expressed in conditions that**

91 **triggered cell differentiation and sexual reproduction and are of red algal origin.**

92

93 **S6 Fig. Expression values (FPKM) of 15 selected genes across the three growth phases for**

94 **each nitrogen treatment.**

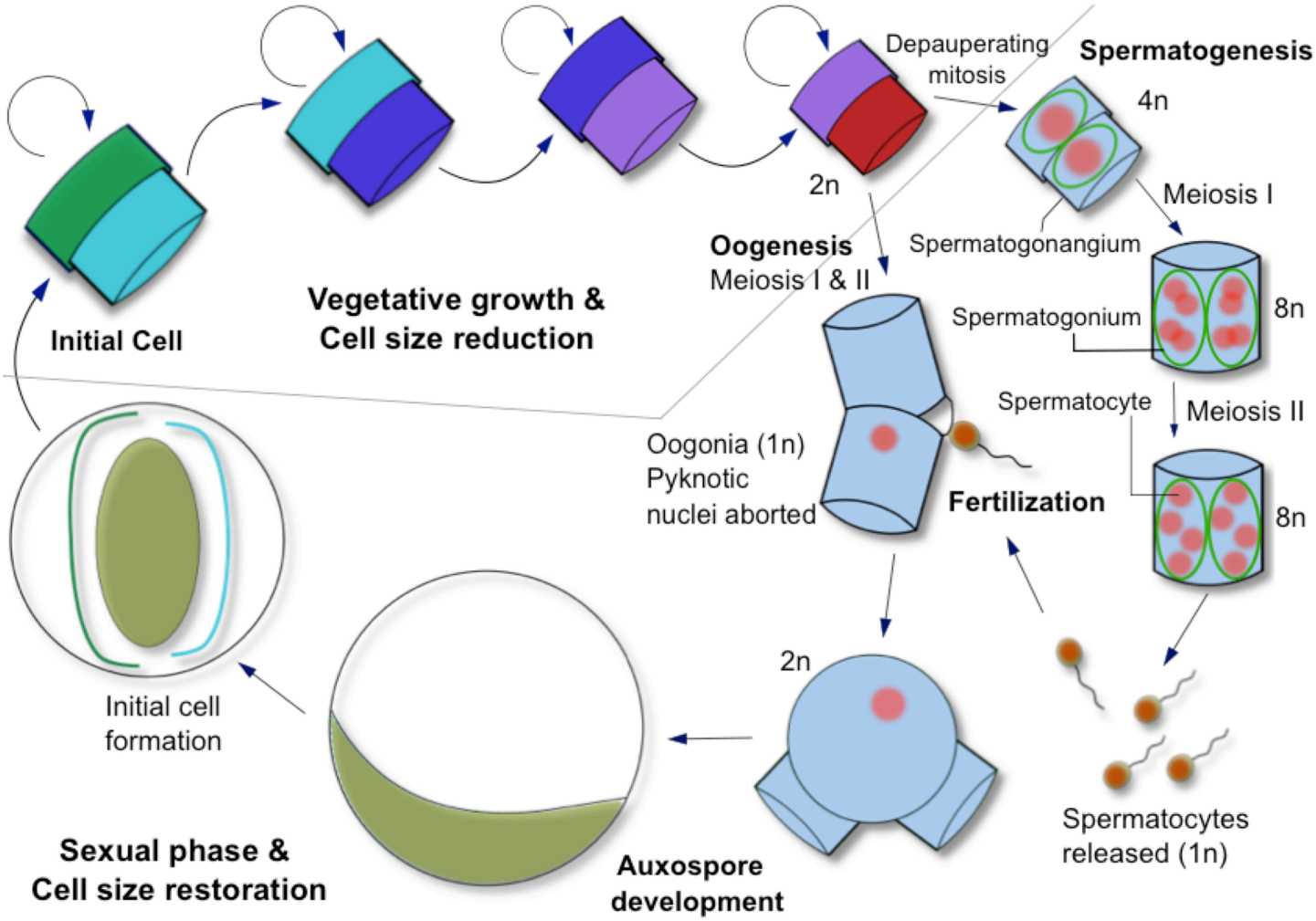
Depauperating mitosis
Spermatogenesis
4n
2n
Meiosis I
Oogenesis
Meiosis I & II
Spermatogonangium
Spermatogonium
8n
Initial Cell
Vegetative growth &
Cell size reduction
Spermatocyte
Meiosis II
Oogonia (1n)
Pyknotic
nuclei aborted
Fertilization
8n
2n
Initial cell
formation
Spermatocytes
released (1n)
Sexual phase &
Cell size restoration
Auxospore
development

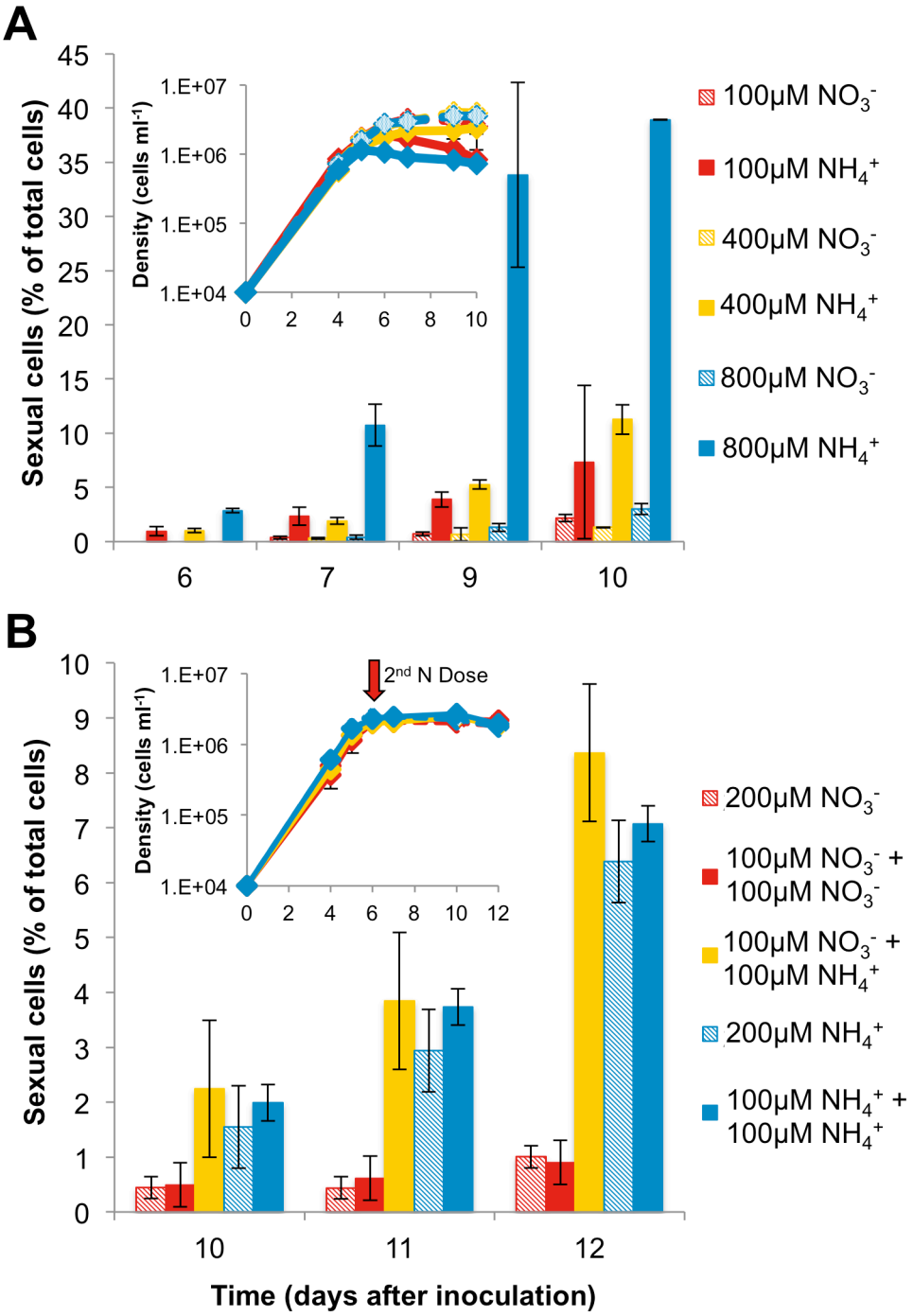
A
Sexual cells (% of total cells)
45
40
35
30
25
20
15
10
5
0
6
7
9
10
Density (cells ml-1)
1.E+07
1.E+06
1.E+05
1.E+04
0
2
4
6
8
10
100μM NO3-
100μM NH4+
400μM NO3-
400μM NH4+
800μM NO3-
800μM NH4+
B
Sexual cells (% of total cells)
10
9
8
7
6
5
4
3
2
1
0
10
11
12
Time (days after inoculation)
2nd N Dose
Density (cells ml-1)
1.E+07
1.E+06
1.E+05
1.E+04
0
2
4
6
8
10
12
200μM NO3-
100μM NO3- + 100μM NO3-
100μM NO3- + 100μM NH4+
200μM NH4+
100μM NH4+ + 100μM NH4+

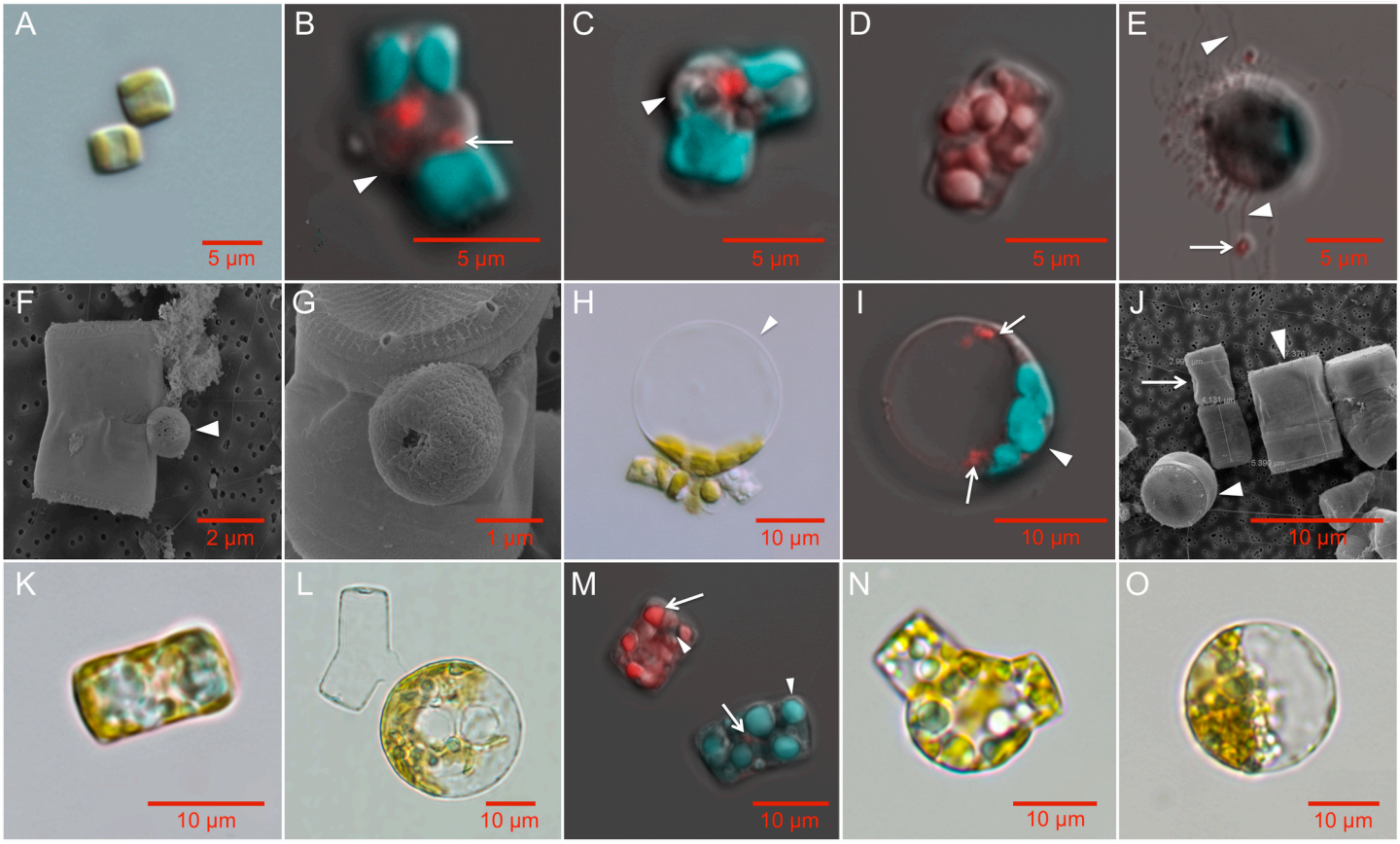
A
5 µm
B
5 µm
C
5 µm
D
5 µm
E
5 µm
F
2 µm
G
1 µm
H
10 µm
I
10 µm
J
10 µm
K
10 µm
L
10 µm
M
10 µm
N
10 µm
O
10 µm

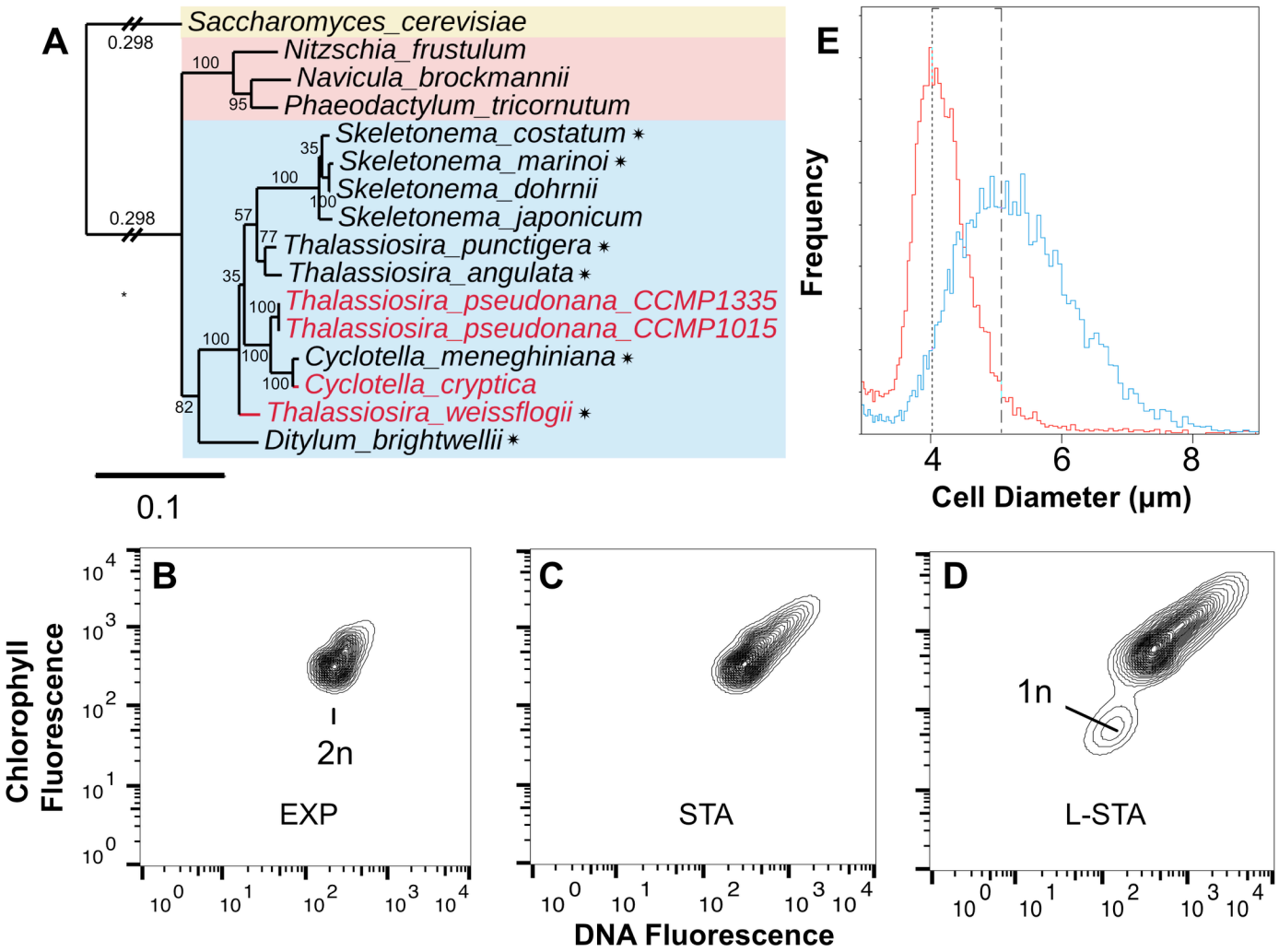
A
Saccharomyces_cerevisiae
Nitzschia_frustulum
Navicula_brockmannii
Phaeodactylum_tricornutum
Skeletonema_costatum
Skeletonema_marinoi
Skeletonema_dohrnii
Skeletonema_japonicum
Thalassiosira_punctigera
Thalassiosira_angulata
Thalassiosira_pseudonana_CCMP1335
Thalassiosira_pseudonana_CCMP1015
Cyclotella_meneghiniana
Cyclotella_cryptica
Thalassiosira_weissflogii
Ditylum_brightwellii
0.298
0.298
0.1
E
Frequency
Cell Diameter (µm)
B
C
D
Chlorophyll Fluorescence
DNA Fluorescence
2n
EXP
STA
1n
L-STA

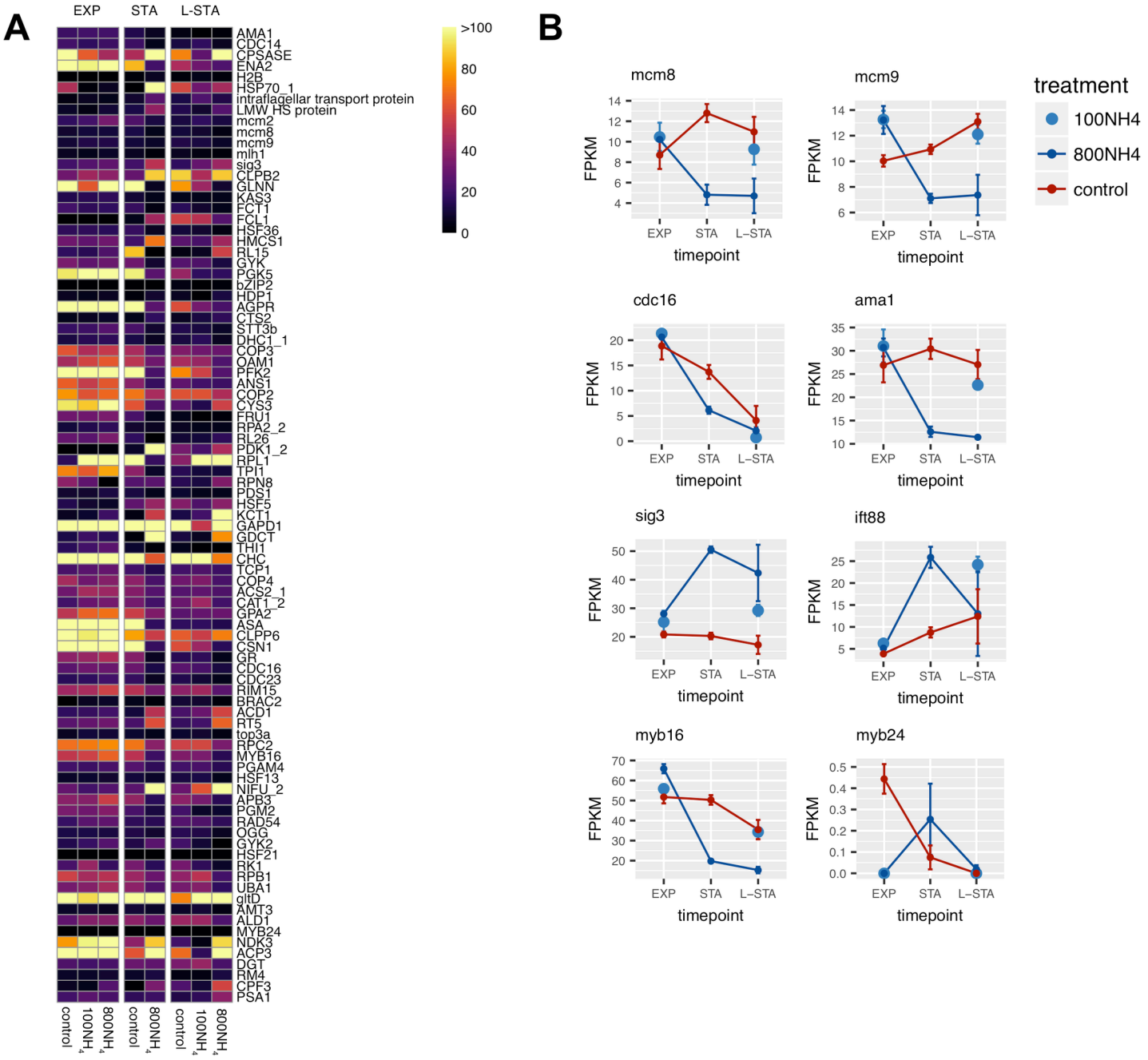
A
EXP
STA
L-STA
AMA1
CDC14
CPSASE
ENA2
H2B
HSP70_1
intraflagellar transport protein
LMW HS protein
mcm2
mcm8
mcm9
mlh1
sig3
CLPB2
GLNN
KAS3
FCT1
FCL1
HSF36
HMCS1
RL15
GYK
PGK5
bZIP2
HDP1
AGPR
CTS2
STT3b
DHC1_1
COP3
OAM1
PFK2
ANS1
COP2
CYS3
FRU1
RPA2_2
RL26
PDK1_2
RPL1
TPI1
RPN8
PDS1
HSF5
KCT1
GAPD1
GDCT
THI1
CHC
TCP1
COP4
ACS2_1
CAT1_2
GPA2
ASA
CLPP6
CSN1
GR
CDC16
CDC23
RIM15
BRAC2
ACD1
RT5
top3a
RPC2
MYB16
PGAM4
HSF13
NIFU_2
APB3
PGM2
RAD54
OGG
GYK2
HSF21
RK1
RPB1
UBA1
gltD
AMT3
ALD1
MYB24
NDK3
ACP3
DGT
RM4
CPF3
PSA1
control
100NH4
800NH4
control
800NH4
control
100NH4
800NH4
>100
80
60
40
20
0
B
mcm8
mcm9
cdc16
ama1
sig3
ift88
myb16
myb24
FPKM
timepoint
EXP
STA
L–STA
treatment
100NH4
800NH4
control